Communications in Physics, Vol. 34, No. 3 (2024), pp. 297-316
DOI: https://doi.org/10.15625/0868-3166/20089

Higgs phenomenology in the flipped 3-3-1 model

P. N. Thu[1,2,†], **N. T. Duy**[3] **and D. T. Huong**[3]

[1]*Graduate University of Science and Technology, Vietnam Academy of Science and Technology, 18 Hoang Quoc Viet, Cau Giay, Hanoi, Vietnam*

[2]*Faculty of Natural Sciences-Technology, Tay Bac University, Quyet Tam Ward, Son La City, Son La, Vietnam*

[3]*Institute of Physics, Vietnam Academy of Science and Technology, 10 Dao Tan, Ba Dinh, Hanoi, Vietnam*

E-mail: [†]phamngocthutb@tbu.edu.vn

Received 5 February 2024
Accepted for publication 3 June 2024
Published 1 August 2024

Abstract. *We investigate the Higgs phenomenology in the flipped 3-3-1 model, assuming the conservation of the $B-L$ number. In addition to heavy scalar particles with masses at the new physics scale, there are three other light Higgs bosons with masses at the electroweak scale, apart from the SM-like Higgs ones. The new neutral CP-even scalar Higgs boson is identified as the scalar Higgs one with a mass of 95 GeV, in a consistency with the observations from CMS experiment. Regarding the light CP-even scalar, we characterize its Higgs coupling properties using a series of strength modifier parameters. These parameters represent the ratios of the Higgs bosons-particle couplings to their corresponding SM values. We examine various decay processes for the light CP-even scalar Higgs boson and find that our numerical analysis aligns with experimental constraints.*

Keywords: Higgs phenomenology; electroweak scale; new physics scale; flipped 3-3-1 model.
Classification numbers: 12.15.-y; 12.60.-i; 12.60.Cn; 14.80.Bn.

1. Introduction

After the discovery of the 125 GeV Higgs boson [1, 2], the question of whether another Higgs scalar exists remains important and unanswered. To clear this point, researchers have extensively probed colliders like LEP, Tevatron, and LHC, unearthing intriguing clues [3–14]. These

searches have provided valuable insights into the quest for new particles and phenomena. The inaugural indication of a lighter Higgs boson surfaced in 2003 when the LEP experiment [4] reported a 2.3σ local excess in the $e^+e^- \to Z(H \to b\bar{b})$ channel with a mass around 98 GeV. Utilizing the complete dataset from the LHC Run II, the CMS collaboration has published results on the search for a low-mass Higgs boson in the di-photon states [15–17]. These results show an excess of events at a mass of about 95 GeV with a local significance of 2.9σ [15]. A CMS search [16] performed at center-of-mass energies of 8 and 13 TeV in the mass range of 70 or 80 GeV $< m_{\gamma\gamma} <$ 110 GeV reported an excess with respect to the SM prediction, maximal for a mass hypothesis of 95.3 GeV, with a local (global) significance of 2.8 σ (1.3 σ). This result is also confirmed by latest CMS report [17]. In addition, there is another CMS seach for Higgs boson by using di-tau final states which shows an excess compatible with a mass of 95 GeV [14]. This suggests the potential existence of an undiscovered light scalar particle with a mass around 95 GeV.

In fact, many generalized models also include additional scalar fields such as the Two Higgs Doublet Models (2HDMs) [18–20], the Three Higgs Doublet Models (3HDMs) [21, 22], Next-to-Minimal Supersymmetric Models (NMSSM) [23], and models based on the extension of the gauge symmetry group of the SM [24–28]. Among this class of models, those based on the gauge symmetry group $SU(3)_C \times SU(3)_L \times U(1)_X$ (so-called 331 models) [29–34], are of interest because the 3-3-1 models can account for the existence of only three fermions [30, 32], strong CP conservation [35–37], and electric charge quantization [38–41], as well as dark matter [42–45], neutrino masses [46–48], cosmic inflation, and matter-antimatter asymmetry [49–51]. We would like to note that in the 3-3-1 models closely related to the $SU(3)_L^3$ anomaly, the arrangement of fermions follows a specific pattern: the number of fermion multiplets equals that of the anti-multiplets. The most common approach is to organize all three generations of fermions, with one generation of quarks transforming as triplets under the $SU(3)_L$ symmetry, while the two remaining quark generations transform as anti-triplets.

Recently, Fonseca and Hirch [52] showed that the $[SU(3)_L]^3$ anomaly ($\mathscr{A}$) induced by a fermion sextet is related to that induced by a fermion triplet as $\mathscr{A}(6) = 7\mathscr{A}(3)$. Therefore, the $[SU(3)_L]^3$ anomaly can be eliminated if one places a lepton generation in a sextet, two other lepton generations in triplets, and arranges three quark generations in anti-triplets. Due to the interchange of quark and lepton representations, the 3-3-1 model is termed the flipped 3-3-1 model (F331M). Flavor-changing processes in the quark sectors [53–60] are converted into the lepton sector [61–64]. Additionally, research in [61] has shown that the F331M can be an effective theory of a manifest $B-L$ symmetry at high energy, analogous to the standard model. In this theory, it is shown that the additional symmetry can resolve unwanted vacuum expectation values (VEVs) and interactions, which otherwise might lead to significant flavor-changing neutral currents (FCNCs) in the lepton sector. The F331M consists of three scalar triplets and one scalar sextet, which includes three doublet Higgs with three VEVs that break the $SU(2)_L \times U(1)_X$ symmetry. Consequently, the scalar sector is expected to account for an excess of events at a mass of approximately 95 GeV. The properties of the SM-like Higgs boson may differ from those of the SM Higgs boson. In this work, we focus on studying in detail the scalar sector in the F331M, especially the production and decay of the SM-like Higgs boson, as well as the production of the 95 GeV scalar associated with its decay to diphoton.

The paper is organized as follows: In Sec. 2, we review the key features of the F331M and delve into a detailed study of the Higgs sector. The properties of the SM-like Higgs boson, denoted

by h, are discussed in Sec. 4. Sec. 5 analyzes the implications of the model for the observed 95 GeV diphoton excess. Finally, Sec. 6 presents our concluding remarks.

2. The F331 model

The F331M is based on the gauge symmetry described by

$$SU(3)_C \otimes SU(3)_L \otimes U(1)_X, \tag{1}$$

where the first factor, $SU(3)_C$, is the familiar symmetry group of QCD. The remaining, $SU(3)_L$ and $U(1)_X$ represent non-trivial extensions of the electroweak symmetry group. The electric charge (Q) and hypercharge (Y) are embedded through the following relations:

$$Q = T_3 + \beta T_8 + X, \quad Y = \beta T_8 + X, \tag{2}$$

where T_n $(n = 1,2,3,...,8)$ represent the generators of the $SU(3)_L$ group, and X is the generator of the $U(1)_X$ group. While the coefficient β sets the electric charge of new particles, its theoretical values remain undetermined. Unlike other parameters constrained by anomalies, β is free to take any value and determines the electric charge of the new particle. One possible parametrization, as suggested in [63], $\beta = -(2q+1)/\sqrt{3}$, expresses the left-handed fermion representations under $SU(3)_L$ are generally given by

$$\psi_{1L} = \begin{pmatrix} \xi_1^{-q} & \frac{1}{\sqrt{2}}\xi_2^{-1-q} & \frac{1}{\sqrt{2}}\nu_1 \\ \frac{1}{\sqrt{2}}\xi_2^{-1-q} & \xi_3^{-2-q} & \frac{1}{\sqrt{2}}e_1 \\ \frac{1}{\sqrt{2}}\nu_1 & \frac{1}{\sqrt{2}}e_1 & k_1^q \end{pmatrix}_L \sim 3, \tag{3}$$

$$\psi_{\alpha L} = \begin{pmatrix} \nu_\alpha \\ e_\alpha \\ k_\alpha^q \end{pmatrix}_L \sim 3, \quad Q_{aL} = \begin{pmatrix} d_a \\ -u_a \\ j_a^{-q-1/3} \end{pmatrix}_L \sim 3^*. \tag{4}$$

It is worth noting that the generation indexes used here are $a = 1,2,3$, and $\alpha = 2,3$. Additionally, all right-handed fermions are singlets under the $SU(3)_L$ group. An interesting exception arises when $\beta = \frac{1}{\sqrt{3}}$. In this specific case, as detailed in (see in [63]), the right-handed ξ_{iR}, E_{iR} can be omitted as ν_{aR}. This simplification results in more economical fermion content, as follows:

$$\psi_{1L} = \begin{pmatrix} \xi^+ & \frac{1}{\sqrt{2}}\xi^0 & \frac{1}{\sqrt{2}}\nu_1 \\ \frac{1}{\sqrt{2}}\xi^0 & \xi^- & \frac{1}{\sqrt{2}}e_1 \\ \frac{1}{\sqrt{2}}\nu_1 & \frac{1}{\sqrt{2}}e_1 & E_1 \end{pmatrix}_L \sim \left(1, 6, -\frac{1}{3}\right), \tag{5}$$

$$\psi_{\alpha L} = \begin{pmatrix} \nu_\alpha \\ e_\alpha \\ E_\alpha \end{pmatrix}_L \sim \left(1, 3, -\frac{2}{3}\right), \tag{6}$$

$$e_{aR} \sim (1,1,-1), \quad E_{aR} \sim (1,1,-1), \tag{7}$$

$$Q_{aL} = \begin{pmatrix} d_a \\ -u_a \\ U_a \end{pmatrix}_L \sim \left(3, 3^*, \frac{1}{3}\right), \tag{8}$$

$$u_{aR} \sim (3,1,2/3), \quad d_{aR} \sim (3,1,-1/3), \quad U_{aR} \sim (3,1,2/3). \tag{9}$$

It is important to note that the electric charges of E and U are equivalent to those of the charged leptons and up-quarks, respectively.

The scalar sector, which is responsible for symmetry breaking and mass generation in the F331M, is described as follows:

$$\eta = \begin{pmatrix} \eta_1^0 \\ \eta_2^- \\ \eta_3^- \end{pmatrix} \sim (1,3,-2/3), \quad \rho = \begin{pmatrix} \rho_1^+ \\ \rho_2^0 \\ \rho_3^0 \end{pmatrix} \sim (1,3,1/3), \tag{10}$$

$$\chi = \begin{pmatrix} \chi_1^+ \\ \chi_2^0 \\ \chi_3^0 \end{pmatrix} \sim (1,3,1/3), \quad S = \begin{pmatrix} S_{11}^{++} & \frac{1}{\sqrt{2}}S_{12}^+ & \frac{1}{\sqrt{2}}S_{13}^+ \\ \frac{1}{\sqrt{2}}S_{12}^+ & S_{22}^0 & \frac{1}{\sqrt{2}}S_{23}^0 \\ \frac{1}{\sqrt{2}}S_{13}^+ & \frac{1}{\sqrt{2}}S_{23}^0 & S_{33}^0 \end{pmatrix} \sim (1,6,2/3). \tag{11}$$

Interestingly, the model exhibits a unique feature with the scalar fields ρ and χ. They are identical under the gauge symmetry but possess distinct $B-L$ charges, as detailed in [63]. The specific values of these charges are presented in the following Table 1.

Table 1. $B-L$ charges for each field in the F331M.

Field	e^-	ν	$u^{2/3}$	$d^{-1/3}$	ξ^+	ξ^0	ξ^-	E^-	$U^{2/3}$	X^+	Y^0	ρ_1^+	ρ_2^0
B-L	-1	-1	1/3	1/3	0	0	0	-2	$4/3$	1	1	0	0
Field	ρ_3^0	χ_1^+	χ_2^0	χ_3^0	η_1^0	η_2^-	η_3^-	S_{11}^{++}	S_{12}^+	S_{13}^+	S_{22}^0	S_{23}^0	S_{33}^0
B-L	-1	1	1	0	0	0	-1	0	0	1	0	1	0

3. The Higgs mass spectrums

Based on the above Higgs multiplets, the scalar potential of the model can be described by two key parts as follows

$$\mathscr{V} = V + \not{V}. \tag{12}$$

The first part, denoted by V, is split into two parts as follows:

$$V = V_1 + V_2, \tag{13}$$

with

$$\begin{aligned} V_1 \;=\; & \mu_\eta^2 \eta^\dagger\eta + \mu_\rho^2 \rho^\dagger\rho + \mu_\chi^2 \chi^\dagger\chi + \mu_S^2 \mathrm{Tr}(S^\dagger S) \\ & + \lambda_\eta (\eta^\dagger\eta)^2 + \lambda_\rho (\rho^\dagger\rho)^2 + \lambda_\chi \left(\chi^\dagger\chi\right)^2 + \lambda_{1S}\mathrm{Tr}^2(S^\dagger S) + \lambda_{2S}\mathrm{Tr}(S^\dagger S)^2 \\ & + \lambda_{\eta\rho}(\eta^\dagger\eta)(\rho^\dagger\rho) + \lambda_{\chi\eta}(\chi^\dagger\chi)(\eta^\dagger\eta) + \lambda_{\chi\rho}(\chi^\dagger\chi)(\rho^\dagger\rho) \\ & + \lambda_{\eta S}(\eta^\dagger\eta)\mathrm{Tr}(S^\dagger S) + \lambda_{\rho S}(\rho^\dagger\rho)\mathrm{Tr}(S^\dagger S) + \lambda_{\chi S}(\chi^\dagger\chi)\mathrm{Tr}(S^\dagger S) \\ & + \lambda'_{\eta\rho}(\eta^\dagger\rho)(\rho^\dagger\eta) + \lambda'_{\chi\eta}(\chi^\dagger\eta)(\eta^\dagger\chi) + \lambda'_{\chi\rho}(\chi^\dagger\rho)(\rho^\dagger\chi) \\ & + \lambda'_{\chi S}(\chi^\dagger S)(S^\dagger\chi) + \lambda'_{\eta S}(\eta^\dagger S)(S^\dagger\eta) + \lambda'_{\rho S}(\rho^\dagger S)(S^\dagger\rho) \\ & + \left(\mu\eta\rho\chi + \mu'\chi^T S^*\chi + H.c.\right). \end{aligned} \tag{14}$$

Here the couplings λ's are dimensionless, while the parameters μ's have mass dimension,

$$\begin{aligned} V_2 &= \lambda_{\chi\rho\eta}(\chi^\dagger\rho)(\eta^\dagger\eta)+\lambda_{\chi\rho\rho}(\chi^\dagger\rho)(\rho^\dagger\rho)+\lambda_{\chi\rho\eta}(\chi^\dagger\rho)(\eta^\dagger\eta) \\ &\quad +\lambda_{\chi\rho S}(\chi^\dagger\rho)\mathrm{Tr}(S^\dagger S)+\lambda'_{\chi\rho S}(\chi^\dagger S)(S^\dagger\rho)+H.c. \end{aligned} \tag{15}$$

The second part, denoted by $\not{V}$, contains the unwanted interactions between the scalar fields, ρ,χ, and S. These interactions might lead to undesirable phenomena in the model and they have the following form as

$$\not{V} = f^2\rho^\dagger\chi+f'\rho^T S^*\chi+f''\rho^T S^*\rho+H.c., \tag{16}$$

where f's are mass parameters analogous to μ's. The theory may contain hidden symmetries which suppress these unwanted terms at low energy, we can safely ignore them in our studies at such energy scales. Here, the $U(1)_N$ symmetry emerges as a potential hidden symmetry that can suppress the unwanted interactions. The $N-$charge, associated with the $U(1)_N$ symmetry, determines the $B-L$ charge of a particle through the following relation:

$$B-L=\frac{2}{\sqrt{3}}T_8+N. \tag{17}$$

In the Table 2, we list the specific $N-$charges assigned to the various particle multiplets in the F331M.

Table 2. $N-$charge of particle multiplets.

Multiplet	ψ_{1L}	$\psi_{\alpha L}$	Q_{aL}	ν_{aR}	e_{aR}	E_{aR}	u_{aR}	d_{aR}	U_{aR}	ρ	χ	η	S	ϕ
N	$-\frac{2}{3}$	$-\frac{4}{3}$	$\frac{2}{3}$	-1	-1	-2	$\frac{1}{3}$	$\frac{1}{3}$	$\frac{4}{3}$	$-\frac{1}{3}$	$\frac{2}{3}$	$-\frac{1}{3}$	$\frac{4}{3}$	2

We expand the neutral scalar components of the scalar multiplets around their VEVs as follows:

$$\begin{aligned} \eta_1^0 &= \frac{1}{\sqrt{2}}(u+S_1+iA_1), \quad \rho_2^0=\frac{1}{\sqrt{2}}(v+S_2+iA_2), \quad \rho_3^0=\frac{1}{\sqrt{2}}(S_3+iA_3), \\ \chi_2^0 &= \frac{1}{\sqrt{2}}(S_4+iA_4), \quad \chi_3^0=\frac{1}{\sqrt{2}}(w+S_5+iA_5), \quad S_{22}^0=\frac{1}{\sqrt{2}}(\kappa+S_6+iA_6), \\ S_{23} &= \frac{1}{\sqrt{2}}(S_7+iA_7), \quad S_{33}=\frac{1}{\sqrt{2}}(\Lambda+S_8+iA_8). \end{aligned}$$

Noting that the $B-L$ symmetry preserves the vacuum state, only scalar fields with even $B-L$ charges can develop the VEVs. The extreme condition of the scalar potential, expressed as $\frac{\partial V}{\partial S_i}=0$

for all scalar fields S_i, leads to the following system of equations

$$\begin{aligned}
&\mu_\eta^2+\frac{\lambda_{\eta S}u\kappa^2+\lambda_{\eta S}\Lambda^2u+\lambda_{\chi\eta}uw^2+2\lambda_\eta u^3+\lambda_{\eta\rho}uv^2+\sqrt{2}\mu vw}{2u}=0,\\
&\mu_\rho^2+\frac{\left((\lambda'_{\rho S}+\lambda_{\rho S})\kappa^2+\Lambda^2\lambda_{\rho S}+\lambda_{\chi\rho}w^2+\lambda_{\eta\rho}u^2\right)v+2\lambda_\rho v^3+\sqrt{2}\mu uw}{2v}=0,\\
&\mu_\chi^2+\frac{w\left(\lambda_{\chi S}\kappa^2+\left((\lambda_{\chi S}\Lambda+\lambda'_{\chi S})+2\sqrt{2}\mu'\right)+2\lambda_\chi w^2+\lambda_{\chi\eta}u^2+\lambda_{\chi\rho}v^2\right)\Lambda+\sqrt{2}\mu uv}{2w}=0,\\
&\mu_S^2+\frac{\sqrt{2}f''v^2+2\lambda_{1S}\kappa^3+2\lambda_{2S}\kappa^3+2\lambda_{1S}\kappa\Lambda^2+\kappa\lambda_{\chi S}w^2+\lambda_{\eta S}\kappa u^2+\lambda'_{\rho S}\kappa v^2+\lambda_{\rho S}\kappa v^2}{2\kappa}=0,\\
&\mu'+\frac{-2f''\Lambda v^2-2\sqrt{2}\lambda_{2S}\kappa^3\Lambda+2\sqrt{2}\lambda_{2S}\kappa\Lambda^3+\sqrt{2}\kappa\Lambda\lambda'_{\chi S}w^2-\sqrt{2}\lambda'_{\rho S}\kappa\Lambda v^2}{2\kappa w^2}=0. \qquad (18)
\end{aligned}$$

After substituting the extreme conditions into the Higgs potential, we obtain the mass spectrum of the particles which are shown below.

3.1. The CP-even scalar sector

The theory contains eight CP-even scalar fields. Five of them, S_1,S_2,S_5,S_6,S_8, have zero $B-L$ quantum numbers, while the remaining fields, S_3,S_4,S_7, have non-zero $B-L$ quantum numbers. Fields carrying the same $B-L$ quantum numbers mix. In the system (S_1,S_2,S_5,S_6,S_8) the mass mixing matrix is represented as follows:

$$M_S^2=\begin{pmatrix}
2\lambda_\eta u^2-\frac{\mu vw}{\sqrt{2}u} & \lambda_{\eta\rho}uv+\frac{\mu w}{\sqrt{2}} & \lambda_{\chi\eta}uw+\frac{\mu v}{\sqrt{2}} & \kappa\lambda_{\eta S}u & \Lambda\lambda_{\eta S}u\\
\lambda_{\eta\rho}uv+\frac{\mu w}{\sqrt{2}} & 2\lambda_\rho v^2-\frac{\mu uw}{\sqrt{2}v} & \lambda_{\chi\rho}vw+\frac{\mu u}{\sqrt{2}} & \kappa v(\lambda'_{\rho S}+\lambda_{\rho S}) & \Lambda\lambda_{\rho S}v\\
\lambda_{\chi\eta}uw+\frac{\mu v}{\sqrt{2}} & \lambda_{\chi\rho}vw+\frac{\mu u}{\sqrt{2}} & 2\lambda_\chi w^2-\frac{\mu uv}{\sqrt{2}w} & \kappa\lambda_{\chi S}w & (M_S^2)_{36}\\
k\lambda_{\eta S}u & kv(\lambda'_{\rho S}+\lambda_{\rho S}) & k\lambda_{\chi S}w & 2\kappa^2(\lambda_{1S}+\lambda_{2S}) & 2k\lambda_{1S}\Lambda\\
\Lambda\lambda_{\eta S}u & \Lambda\lambda_{\rho S}v & (M_S^2)_{36} & 2k\lambda_{1S}\Lambda & (M_S^2)_{66}
\end{pmatrix}, \qquad (19)$$

where the matrix elements $(M_S^2)_{33,66}$ are given by

$$\begin{aligned}
(M_S^2)_{36}&=\frac{\Lambda\left(2\kappa^2\lambda_{2S}-2\lambda_{2S}\Lambda^2+\lambda_{\chi S}w^2+\lambda'_{\rho S}v^2\right)}{w},\\
(M_S^2)_{66}&=\frac{-2\kappa^2\lambda_{2S}+4\lambda_{1S}\Lambda^2+6\lambda_{2S}\Lambda^2+\lambda'_{\chi S}w^2-\lambda'_{\rho S}v^2}{2}. \qquad (20)
\end{aligned}$$

Before breaking the electroweak symmetry, the mass matrix shown above has the simple form:

$$M_{0S}^2=\begin{pmatrix}
-\frac{\mu w}{\sqrt{2}t} & \frac{\mu w}{\sqrt{2}} & 0 & 0 & 0\\
\frac{\mu w}{\sqrt{2}} & -\frac{\mu tw}{\sqrt{2}} & 0 & 0 & 0\\
0 & 0 & 2\lambda_\chi w^2 & 0 & \lambda_{\chi S}\Lambda w-\frac{2\lambda_{2S}\lambda^3}{w}\\
0 & 0 & 0 & 0 & 0\\
0 & 0 & \lambda_{\chi S}\Lambda w-\frac{2\lambda_{2S}\lambda^3}{w} & 0 & (2\lambda_{1S}+3\lambda_{2S})\lambda^2+\frac{\lambda'_{\chi S}w^2}{2}
\end{pmatrix}, \qquad (21)$$

where $t=\frac{u}{v}$. This matrix identifies two massless fields: one is identified as the SM-like Higgs boson (h^0) and another identified as the 95 GeV Higgs boson (h_{95}^0), potentially beyond the SM.

There are also three massive Higgs boson fields with masses at the new physics scale, denoted as H_1^0, H_2^0, and H_3^0. After electroweak symmetry breaking: there is an additional mixing term appeared, $\Delta M_S^2 = M_S^2 - M_{0S}^2$. Assuming, $w, \Lambda \gg u, v, \kappa$, the term ΔM_S^2 is known as a "perturbing" squared mass term. Up to the first-order perturbation, the expressions for the squared masses are

$$\begin{aligned} m_{h_{95}}^2 &= \left\{ \frac{t'^2\left(t^2+1\right)(\lambda_{1S}+\lambda_{2S}) + \lambda_\eta t^4 + \lambda_{\eta\rho} t^2 + \lambda_\rho - \lambda_{\text{eff}}}{t^2+1} \right\} v^2, \\ m_h^2 &= \left\{ \frac{t'^2\left(t^2+1\right)(\lambda_{1S}+\lambda_{2S}) + \lambda_\eta t^4 + \lambda_{\eta\rho} t^2 + \lambda_\rho + \lambda_{\text{eff}}}{t^2+1} \right\} v^2, \end{aligned} \tag{22}$$

$$m_{H_1}^2 = -\frac{\mu w \tan\alpha}{\sqrt{2}} + \mathscr{O}(u, v, \kappa), \tag{23}$$

$$m_{H_2}^2 = 2(2\lambda_{1S}\Lambda^2 + 3\lambda_{2S}) + (4\lambda_\chi + \lambda'_{\chi S})w^2 - \frac{\Delta}{4w} + \mathscr{O}(u, v, \kappa), \tag{24}$$

$$m_{H_3}^2 = 2(2\lambda_{1S} + 3\lambda_{2S})\Lambda^2 + (4\lambda_\chi + \lambda'_{\chi S})w^2 + \frac{\Delta}{4w} + \mathscr{O}(u, v, \kappa), \tag{25}$$

with $t' = \frac{\kappa}{v}$, and

$$\begin{aligned} \lambda_{\text{eff}}^2 &= \left(t^2+1\right)t'^2\left(t^4\left(\lambda_{\eta S}^2 - 2\lambda_\eta(\lambda_{1S}+\lambda_{2S})\right) + 2\lambda_{\eta S}t^2(\lambda'_{\rho S}+\lambda_{\rho S}) + (\lambda'_{\rho S}+\lambda_{\rho S})^2\right) \\ &+ \left(t^2+1\right)^2 t'^4(\lambda_{1S}+\lambda_{2S})^2 + \left(\lambda_\eta t^4 + \lambda_{\eta\rho}t^2 + \lambda_\rho\right)^2 - 2(\lambda_{1S}+\lambda_{2S})\left(\lambda_{\eta\rho}t^2+\lambda_\rho\right), \end{aligned} \tag{26}$$

$$\begin{aligned} \Delta^2 &= 4\left((2\lambda_{1S}+3\lambda_{2S})^2 - 16\lambda_{2S}\lambda_{\chi S}\right)\Lambda^4 w^2 + 4\left((2\lambda_{1S}+3\lambda_{2S})(\lambda'_{\chi S}-4\lambda_\chi) + 4\lambda_{\chi S}^2\right)\Lambda^2 w^4 \\ &+ 64\lambda_{2S}^2\Lambda^6 + (\lambda'_{\chi S}-4\lambda_\chi)^2 w^6, \end{aligned} \tag{27}$$

and their eigenstates are given, respectively

$$\begin{pmatrix} h \\ h_{95} \\ H_1 \\ H_2 \\ H_3 \end{pmatrix} = \begin{pmatrix} \sin\alpha\sin\gamma_1 & \cos\alpha\sin\gamma_1 & \cos\gamma_1 & 0 & 0 \\ \sin\alpha\sin\gamma_2 & \cos\alpha\sin\gamma_2 & \cos\gamma_2 & 0 & 0 \\ \cos\alpha & -\sin\alpha & 0 & 0 & 0 \\ 0 & 0 & 0 & \sin\beta & \cos\beta \\ 0 & 0 & 0 & \cos\beta & -\sin\beta \end{pmatrix} \begin{pmatrix} S_1 \\ S_2 \\ S_6 \\ S_5 \\ S_8 \end{pmatrix}, \tag{28}$$

where

$$\tan\alpha = \frac{u}{v}, \quad \tan 2\beta = \frac{8\lambda_{2S}\Lambda^3 - 4\lambda_{\chi S}\Lambda w^2}{(4\lambda_\chi - \lambda'_{\chi S})w^3 - 2(2\lambda_{1S}+3\lambda_{2S})\Lambda^2 w},$$

$$\begin{aligned}
\tan\gamma_1 &= \frac{\sqrt{t^2+1}t'\left(\lambda_{\eta S}t^2+\lambda'_{\rho S}+\lambda_{\rho S}\right)}{(t^2+1)t'^2(\lambda_{1S}+\lambda_{2S})+\lambda_\eta t^4+\lambda_{\eta\rho}t^2+\lambda_\rho-2\left(\lambda_\eta t^4+\lambda_{\eta\rho}t^2+\lambda_\rho\right)+\lambda_{\text{eff}}},\\
\tan\gamma_2 &= \frac{\sqrt{t^2+1}t'\left(\lambda_{\eta S}t^2+\lambda'_{\rho S}+\lambda_{\rho S}\right)}{(t^2+1)t'^2(\lambda_{1S}+\lambda_{2S})+\lambda_\eta t^4+\lambda_{\eta\rho}t^2+\lambda_\rho-2\left(\lambda_\eta t^4+\lambda_{\eta\rho}t^2+\lambda_\rho\right)-\lambda_{\text{eff}}}.
\end{aligned} \tag{29}$$

In this work, we assume that the lightest CP-even scalar field, h_{95}, corresponds to a particle with a mass of 95 GeV, aligning with the potential scalar resonance observed by CMS and ATLAS [14–16]. We further identify h with the well-established 125 GeV Higgs boson discovered at the LHC [1,2].

The CP-even scalar fields carrying non-zero $B-L$ quantum numbers S_3,S_4,S_7, mix together. Their mixing matrix results in a massless neutral scalar, identified as the real component of the Goldstone boson $G_{\Re Y^0}$, which is eaten by the complex gauge boson Y, contributing to its mass. Additionally, two massive Higgs fields, H_4^0,H_5^0, emerge from this mixing. At the leading order of approximation, we can derive the properties of these physical states.

$$H_4 \simeq S_3, \quad H_5 \simeq -\cos\xi S_4+\sin\xi S_7, \quad G_{\Re Y^0} \simeq \sin\xi S_4+\cos\xi S_7, \tag{30}$$

with $\tan\xi=\frac{w}{\sqrt{2}\Lambda}$, and their masses are given as follows

$$m^2_{H_4} \simeq \frac{1}{2}\left(\lambda'_{\rho S}\Lambda^2+\lambda'_{\chi\rho}w^2-\sqrt{2}t\mu w\right)+\mathscr{O}(u,v,\kappa), \tag{31}$$

$$m^2_{H_5} \simeq \frac{\left(4\lambda_{2S}\Lambda^2+\lambda'_{\chi S}w^2\right)\left(2\Lambda^2+w^2\right)}{4w^2}+\mathscr{O}(u,v,\kappa). \tag{32}$$

3.2. The CP-odd scalar sector

Within the spectrum of the CP-odd neutral Higgs bosons, five scalar fields (A_1,A_2,A_5,A_6,A_8) carry zero $B-L$ quantum numbers, while the remaining fields (A_3,A_4,A_7) carry non-zero $B-L$ quantum numbers. Consequently, we can divide the mass mixing matrix for the CP-odd scalar sector into two submatrices. For the system consisting of fields (A_1,A_2,A_5,A_6,A_8), the mass mixing matrix takes the form

$$M^2_{A1}=\begin{pmatrix}
-\frac{\mu vw}{\sqrt{2}u} & -\frac{\mu w}{\sqrt{2}} & -\frac{\mu v}{\sqrt{2}} & 0 & 0\\
-\frac{\mu w}{\sqrt{2}} & -\frac{\mu uw}{\sqrt{2}v} & -\frac{\mu u}{\sqrt{2}} & 0 & 0\\
-\frac{\mu v}{\sqrt{2}} & -\frac{\mu u}{\sqrt{2}} & (M^2_{A1})_{33} & 0 & (M^2_{A1})_{35}\\
0 & 0 & 0 & 0 & 0\\
0 & 0 & (M^2_{A1})_{35} & 0 & (M^2_{A1})_{55}
\end{pmatrix}, \tag{33}$$

where matrix elements $(M^2_{A1})_{33,35,55}$ read

$$\begin{aligned}
(M^2_{A1})_{33} &= -\frac{8\kappa^2\lambda_{2S}\Lambda^2 - 8\lambda_{2S}\Lambda^4 + 4\Lambda^2\lambda'_{\rho S}v^2 + \sqrt{2}\mu uvw - 4\Lambda^2\lambda'_{\chi S}w^2}{2w^2},\\
(M^2_{A1})_{35} &= \frac{\Lambda\left(2\kappa^2\lambda_{2S} - 2\lambda_{2S}\Lambda^2 - \lambda'_{\chi S}w^2 + \lambda'_{\rho S}v^2\right)}{w},\\
(M^2_{A1})_{55} &= \frac{-2\kappa^2\lambda_{2S} + 2\lambda_{2S}\Lambda^2 + \lambda'_{\chi S}w^2 - \lambda'_{\rho S}v^2}{2}.
\end{aligned} \tag{34}$$

This matrix yields two massless eigenstates corresponding to the Goldstone bosons of gauges boson Z, Z', along with three massive fields denoted $\mathscr{A}_1, \mathscr{A}_2$, and $\mathscr{A}_3$. The physical states are defined as follows

$$\begin{aligned}
G_Z &\simeq \sin\theta_1 A_1 + \cos\theta_1 A_2, \quad G_{Z'} = A_6 \quad \mathscr{A}_2 \simeq \sin\theta_2 A_5 + \cos\theta_2 A_8,\\
\mathscr{A}_1 &\simeq \cos\theta_1 A_1 - \sin\theta_1 A_2, \quad \mathscr{A}_3 \simeq \cos\theta_2 A_5 - \sin\theta_2 A_8,
\end{aligned} \tag{35}$$

where $\tan\theta_1 = -\frac{u}{v}, \tan\theta_2 = \frac{4\Lambda w}{(-4\Lambda^2+w^2)\left(2\lambda_{2S}\Lambda^2+\lambda'_{\chi S}w^2\right)}$, and their masses are respectively given

$$m^2_{G_Z} = 0, \quad m^2_{G_{Z'}} = 0, \quad m^2_{\mathscr{A}_1} \simeq -\frac{\mu\left(t^2+1\right)w}{\sqrt{2}t}, \tag{36}$$

$$m^2_{\mathscr{A}_2} \simeq \kappa_A - \sqrt{\kappa_A^2 + \frac{-4\Lambda^2+w^2}{2(4\Lambda^2+w^2)}\kappa_A\kappa_B - \kappa_B^2} + \mathscr{O}(u,v,\kappa), \tag{37}$$

$$m^2_{\mathscr{A}_3} \simeq \kappa_A + \sqrt{\kappa_A^2 + \frac{-4\Lambda^2+w^2}{2(4\Lambda^2+w^2)}\kappa_A\kappa_B - \kappa_B^2} + \mathscr{O}(u,v,\kappa), \tag{38}$$

with

$$\kappa_A = \frac{4\Lambda^2+w^2}{4w^2}(2\lambda_{2S}\Lambda^2 + \lambda'_{\chi S}w^2), \quad \kappa_B = \frac{\sqrt{2}\mu uv}{4w}. \tag{39}$$

Three remaining fields (A_3, A_4, A_7) have non-zero $B-L$ quantum numbers, so they are mixed.

$$M^2_{A2} = \begin{pmatrix}
\frac{1}{2}\left(\lambda'_{\rho S}(\Lambda^2-\kappa^2) + \left(\lambda'_{\chi\rho}w - \sqrt{2}\mu t\right)w\right) & \frac{\sqrt{2}\mu u - \lambda'_{\chi\rho}vw}{2} & \frac{\lambda'_{\rho S}v(\kappa-\Lambda)}{2\sqrt{2}}\\
\frac{\sqrt{2}\mu u - \lambda'_{\chi\rho}vw}{2} & (M^2_{A2})_{22} & (M^2_{A2})_{23}\\
\frac{\lambda'_{\rho S}v(\kappa-\Lambda)}{2\sqrt{2}} & (M^2_{A2})_{23} & (M^2_{A2})_{33}
\end{pmatrix}, \tag{40}$$

where the matrix elements $(M_{A2})^2_{22,23,33}$ are given by

$$\begin{aligned}
(M^2_{A2})_{22} &= \frac{2(\Lambda+\kappa)[2\lambda_{2S}(\lambda^2-\kappa^2) - 2\lambda'_{\rho S}v^2]\Lambda + [\lambda'_{\chi S}(\Lambda+\kappa)^2 + \lambda'_{\chi\rho}v^2]w^2 - \sqrt{2}\mu uvw}{2w^2},\\
(M^2_{A2})_{23} &= \frac{-4\lambda_{2S}(\lambda^2-\kappa^2)\Lambda + 2\lambda'_{\rho S}v^2\Lambda - \lambda'_{\chi S}w^2(\Lambda+\kappa)}{2\sqrt{2}w},\\
(M^2_{A2})_{33} &= \frac{4\lambda_{2S}(\Lambda-\kappa)\Lambda + (\lambda'_{\chi S}w^2 - \lambda'_{\rho S}v^2)}{4}.
\end{aligned} \tag{41}$$

The obtained mass eigenstates from the above matrix include one massless scalar particle identified as an imaginary component of the Goldstone boson, G_{Y^0}. This is eaten by the complex gauge boson, Y^0, contributing to its mass. The remaining two eigenstates correspond to the physical neutral Higgs bosons, denoted as $\mathscr{A}_4, \mathscr{A}_5$. At the leading order of approximation, their masses and relationship to the original states can be derived

$$\begin{aligned} m_{G_{\Im Y^0}} &= 0, && (42)\\ m^2_{\mathscr{A}_4} &\simeq \frac{1}{2}\left(\lambda'_{\rho S}\Lambda^2+\lambda'_{\chi\rho}w^2-\sqrt{2}t\mu w\right)+\mathscr{O}(u,v,\kappa), && (43)\\ m^2_{\mathscr{A}_5} &\simeq \frac{\left(4\lambda_{2S}\Lambda^2+\lambda'_{\chi S}w^2\right)\left(2\Lambda^2+w^2\right)}{4w^2}+\mathscr{O}(u,v,\kappa), && (44) \end{aligned}$$

$$\mathscr{A}_4 \simeq A_3, \quad \mathscr{A}_5 \simeq -\cos\xi A_4+\sin\xi A_7, \quad G_{\Im Y^0} \simeq \sin\xi A_4+\cos\xi A_7. \tag{45}$$

3.3. The charged scalar sector

The model contains six singly charged Higgs: $\eta_2^\pm, \eta_3^\pm, \rho_1^\pm, \chi_1^\pm, S_{12}^\pm, S_{13}^\pm$. Three of these Higgs ($\eta_2^\pm$, $\rho_1^\pm, S_{12}^\pm$) are mixed via the following mass matrix

$$M^2_{C1}=\begin{pmatrix} \frac{\lambda'_{\eta S}\kappa^2u+\lambda'_{\eta\rho}uv^2-\sqrt{2}\mu vw}{2u} & \frac{1}{2}\left(\lambda'_{\eta\rho}uv-\sqrt{2}\mu w\right) & \frac{\lambda'_{\eta S}\kappa u}{2\sqrt{2}} \\ \frac{1}{2}\left(\lambda'_{\eta\rho}uv-\sqrt{2}\mu w\right) & -\frac{\lambda'_{\rho S}\kappa^2v-\lambda'_{\eta\rho}u^2v+\sqrt{2}\mu uw}{2v} & \frac{\lambda'_{\rho S}\kappa v}{2\sqrt{2}} \\ \frac{\lambda'_{\eta S}\kappa u}{2\sqrt{2}} & \frac{\lambda'_{\rho S}\kappa v}{2\sqrt{2}} & \frac{1}{4}\left(\lambda'_{\eta S}u^2-\lambda'_{\rho S}v^2\right). \end{pmatrix}. \tag{46}$$

The calculation results in three eigenvalues

$$\begin{aligned} m^2_{G_W^\pm} &= 0, && (47)\\ m^2_{H_1^\pm} &\simeq \frac{tv^2\left[\lambda'_{\eta\rho}\left(1+t^2\right)^2+\left(\lambda'_{\eta S}-\lambda'_{\rho S}t^2\right)t'^2\right]-\sqrt{2}\mu\left(1+t^2\right)^2w}{t(1+t^2)}+\mathscr{O}\left(\frac{v}{w}\right), && (48)\\ m^2_{H_2^\pm} &\simeq \frac{(\lambda'_{\eta S}t^2-\lambda'_{\rho S})v^2}{2}+\mathscr{O}\left(\frac{v}{w}\right), && (49) \end{aligned}$$

and their corresponding eigenstates are related by

$$\begin{pmatrix} G_W^\pm \\ H_1^\pm \\ H_2^\pm \end{pmatrix}=\begin{pmatrix} \frac{t}{\sqrt{1+t^2}} & \frac{-\cos\sigma_1+\sqrt{2}t'\sin\sigma_1}{\sqrt{1+t^2}} & \frac{-\sqrt{2}t'\cos\sigma_1-\sin\sigma_1}{\sqrt{1+t^2}} \\ \frac{-1}{\sqrt{1+t^2}} & \frac{-t\cos\sigma_1}{\sqrt{1+t^2}} & \frac{-t\sin\sigma_1}{\sqrt{1+t^2}} \\ \frac{-\sqrt{2}tt'}{1+t^2} & \frac{\sqrt{2}t'\cos\sigma_1+(1+t^2)\sin\sigma_1}{1+t^2} & \frac{(1+t^2)\cos\sigma_1+\sqrt{2}t'\sin\sigma_1}{1+t^2} \end{pmatrix}\begin{pmatrix} \eta_2^\pm \\ \rho_1^\pm \\ S_{12}^\pm \end{pmatrix}, \tag{50}$$

with the mixing angle σ_1 are defined by

$$\tan 2\sigma_1=\frac{-2\sqrt{2}t^2t'v^2(\lambda'_{\eta S}+\lambda'_{\rho S})\sqrt{t^2+1}}{2\sqrt{2}\mu\left(t^2+1\right)^2w-tv^2\left[(t^2+1)\left(2\lambda'_{\eta\rho}\left(t^2+1\right)-\lambda'_{\eta S}t^2+\lambda'_{\rho S}\right)-2t'^2(\lambda'_{\eta S}+\lambda'_{\rho S})\right]}. \tag{51}$$

The remaining singly charged Higgs $(\chi_1^{\pm}, \eta_3^{\pm}, S_{13}^{\pm})$ mix via a separate mixing matrix as

$$M_{C2}^2 = \begin{pmatrix} (M_{C2}^2)_{11} & \frac{1}{2}\left(\lambda'_{\chi\eta} uw - \sqrt{2}\mu v\right) & (M_{C2}^2)_{13} \\ \frac{1}{2}\left(\lambda'_{\chi\eta} uw - \sqrt{2}\mu v\right) & \frac{\Lambda^2\lambda'_{\eta S}u + \lambda'_{\chi\eta} uw^2 - \sqrt{2}\mu vw}{2u} & \frac{\Lambda\lambda'_{\eta S}u}{2\sqrt{2}} \\ (M_{C2}^2)_{13} & \frac{\Lambda\lambda'_{\eta S}u}{2\sqrt{2}} & (M_{C2}^2)_{33} \end{pmatrix}, \tag{52}$$

where some matrix elements read

$$\begin{aligned} (M_{C2}^2)_{11} &= \frac{4\lambda_{2S}(-\kappa^2\Lambda^2 + \Lambda^4) + \Lambda^2\lambda'_{\chi S}w^2 - 2\Lambda^2\lambda'_{\rho S}v^2 + \lambda'_{\chi\eta}u^2w^2 - \sqrt{2}\mu uvw}{2w^2}, \\ (M_{C2}^2)_{13} &= -\frac{\Lambda\left(-4\kappa^2\lambda_{2S} + 4\lambda_{2S}\Lambda^2 + \lambda'_{\chi S}w^2 - 2\lambda'_{\rho S}v^2\right)}{2\sqrt{2}w}, \\ (M_{C2}^2)_{33} &= \frac{1}{4}\left(-4\kappa^2\lambda_{2S} + 4\lambda_{2S}\Lambda^2 + \lambda'_{\chi S}w^2 + \lambda'_{\eta S}u^2 - 2\lambda'_{\rho S}.v^2\right) \end{aligned} \tag{53}$$

Diagonalizing the squared matrix M_{C2}^2 produces the following eigenvalues

$$\begin{aligned} m^2_{G_X^{\pm}} &= 0, \\ m^2_{H_3^{\pm}} &\simeq \frac{\left[4\lambda_{2S}t\left(2\Lambda^2 + w^2\right)\Lambda^2 + \lambda'_{\chi S}w^2\right]}{2w^2} \\ &\quad + \frac{v^2\left[-2\lambda'_{\rho S}\left(2\Lambda^2 + w^2\right)^2 + tw\left(\lambda'_{\eta S}w^3 + \Lambda^2\left(-4\sqrt{2}\mu + 4\lambda'_{\chi\eta}tw\right)\right)\right]}{2\left(2\Lambda^2 + w^2\right)w^2}, \\ m^2_{H_4^{\pm}} &\simeq \frac{\Lambda^2\lambda'_{\eta S}t + w\left(-\sqrt{2}\mu + \lambda'_{\chi\eta}tw\right)}{t}, \end{aligned} \tag{54}$$

and corresponding eigenvectors

$$\begin{aligned} G_X^{\pm} &\simeq \frac{-w}{\sqrt{2\Lambda^2 + w^2}}\chi_1^{\pm} + \frac{tv\cos\sigma_2 + \sqrt{2}\Lambda\sin\sigma_2}{\sqrt{2\Lambda^2 + w^2}}\eta_3^{\pm} + \frac{tv\sin\sigma_2 - \sqrt{2}\Lambda\cos\sigma_2}{\sqrt{2\Lambda^2 + w^2}}S_{13}^{\pm}, \\ H_3^{\pm} &\simeq \frac{\sqrt{2}\Lambda}{\sqrt{2\Lambda^2 + w^2}}\chi_1^{\pm} + \frac{w\sin\sigma_2}{\sqrt{2\Lambda^2 + w^2}}\eta_3^{\pm} - \frac{w\cos\sigma_2}{\sqrt{2\Lambda^2 + w^2}}S_{13}^{\pm}, \\ H_4^{\pm} &\simeq \frac{-tvw}{2\Lambda^2 + w^2}\chi_1^{\pm} - \left(\cos\sigma_2 - \frac{\sqrt{2}\Lambda tv\sin\sigma_2}{2\Lambda^2 + w^2}\right)\eta_3^{\pm} - \left(\sin\sigma_2 + \frac{\sqrt{2}\Lambda tv\cos\sigma_2}{\Lambda^2 + w^2}\right)S_{13}^{\pm}, \end{aligned} \tag{55}$$

where

$$\tan 2\sigma_2 = \frac{2tvw^2\Lambda\sqrt{2\Lambda^2 + w^2}\left[\sqrt{2}\left(2\lambda'_{\chi\eta} - \lambda'_{\eta S}\right) - 4\mu\right]}{\kappa_H}, \tag{56}$$

and the parameter, κ_H, is defined as

$$\begin{aligned}\kappa_H &\simeq -4\lambda_{2S}t\Lambda^2\left(2\Lambda^2+w^2\right)^2 \\ &\quad -w^2\left(2\Lambda^2+w^2\right)\left[2\Lambda^2 t\left(\lambda'_{\chi S}-\lambda'_{\eta S}\right)+w\left(tw(\lambda'_{\chi S}-2\lambda'_{\chi\eta})+2\sqrt{2}\mu\right)\right] \\ &\quad +tv^2\left\{tw\left(w^2-2\Lambda^2\right)\left[tw\left(2\lambda'_{\chi\eta}-\lambda'_{\eta S}\right)-2\sqrt{2}\mu\right]+2\lambda'_{\rho S}\left(2\Lambda^2+w^2\right)^2\right\}. \end{aligned} \quad (57)$$

The results above show that $G_W^{\pm}$ and $G_X^{\pm}$ are identified as the Goldstone bosons. These Goldstone bosons are eaten by $W_\mu^{\pm}$ and $X_\mu^{\pm}$ bosons, respectively. In addition, the model predicts one light singly charged Higgs $H_2^{\pm}$ with mass at the electroweak scale v, whereas remaining singly charged Higgs bosons $H_{1,3,4}^{\pm}$ have masses at the TeV scale.

4. The properties of the SM-like Higgs boson

Firstly, we investigate the couplings of the CP-even scalars,h and h_{95}, to the SM fermions. These couplings arise from the Yukawa Lagrangian

$$\begin{aligned}\mathscr{L}_{\text{Yukawa}} &= h^e_{\alpha a}\bar{\psi}_{\alpha L}\rho e_{aR}+h^E_{\alpha a}\bar{\psi}_{\alpha L}\chi E_{aR}+h^E_{1a}\bar{\psi}_{1L}SE_{aR}+h^{\xi}\bar{\psi}^c_{1L}\psi_{1L}S \\ &\quad +h^u_{ab}\bar{Q}_{aL}\rho^* u_{bR}+h^d_{ab}\bar{Q}_{aL}\eta^* d_{bR}+h^U_{ab}\bar{Q}_{aL}\chi^* U_{bR}+H.c. \end{aligned} \quad (58)$$

These interactions describe the couplings between all scalar fields and the SM fermions Here, the couplings of the specific scalar fields, h and h_{95}, to the SM fermions are normalized to the corresponding values in the SM values using the mixing angles $\gamma_{1,2}$ as shown below:

$$\kappa_{hf\bar{f}}=\frac{g_{h\bar{f}f}}{g^{\text{SM}}_{h\bar{f}f}}=\frac{\cos\gamma_2}{\sin(\gamma_2-\gamma_1)}, \quad a_{h_{95}f\bar{f}}=\frac{g_{h_{95}\bar{f}f}}{g^{\text{SM}}_{h\bar{f}f}}=\frac{\cos\gamma_1}{\sin(\gamma_2-\gamma_1)}. \quad (59)$$

Similarly, the couplings of the light CP-even Higgs to the SM gauge bosons ($W^{\pm},Z$) are also normalized to the SM values as shown below

$$\begin{aligned}\kappa_{hW^+W^-} &= \frac{g_{hW^+W-}}{g^{SM}_{hW^+W^-}}\simeq\frac{\cos\gamma_2}{\sin(\gamma_2-\gamma_1)}, \quad a_{h_{95}W^+W^-}=\frac{g_{h_{95}W^+W-}}{g^{SM}_{hW^+W^-}}\simeq\frac{\cos\gamma_1}{\sin(\gamma_2-\gamma_1)}, \\ \kappa_{hZZ} &= \frac{g_{hW^+W-}}{g^{SM}_{hW^+W^-}}\simeq\frac{\cos\gamma_2}{\sin(\gamma_2-\gamma_1)}, \quad a_{h_{95}ZZ}=\frac{g_{h_{95}W^+W-}}{g^{SM}_{hW^+W^-}}\simeq\frac{\cos\gamma_1}{\sin(\gamma_2-\gamma_1)}. \end{aligned}$$

The experimental data constraint the SM Higgs decays into a pair of fermions, leading to the constraint on the coupling parameter $a_{h\bar{f}f}$ is shown in [65] as:

$$\kappa^{\text{exp}}_{h\bar{b}b}=0.91^{\pm 0.17}_{-0.16}, \quad \kappa^{\text{exp}}_{h\bar{\mu}\mu}=0.72^{+0.50}_{-0.72}, \quad \kappa^{\text{exp}}_{h\tau\tau}=0.93^{+0.13}_{-0.13}. \quad (60)$$

Figure 1 shows the correlation between two mixing angles γ_1,γ_2 that ensure consistency of the κ_{hff} values given in Eq. (60). We find the constraints for the mixing angle γ_1 as: $\gamma_1>3$ rad. Furthermore, the discovery of the Higgs particle at the LHC during Run 1 [66, 67] was a major success. The overall signal strengths are fully compatible with the SM expectation, $\mu=1$, with a precision of 6%. For the Higgs boson which decays into two photons, the branching ratio normalized to the SM prediction is determined as

$$\mu_{\gamma\gamma}=\frac{\sigma(pp\to h)}{\sigma(pp\to h)_{\text{SM}}}\times\frac{\text{Br}(h\to\gamma\gamma)}{\text{Br}(h\to\gamma\gamma)_{\text{SM}}}. \quad (61)$$

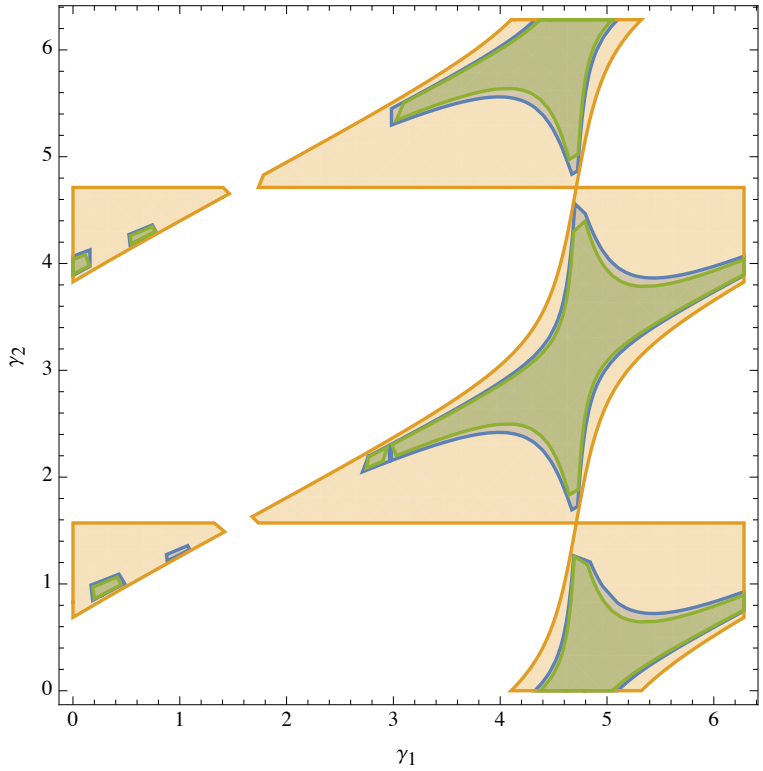

Fig. 1. Correlation between the angles γ_1, γ_2 that are consistent with the experimental constraints given in Eq. (60).

Recently, ATLAS and CMS collaborations [68] have shown the values $\mu_{\gamma\gamma}$ as follows

$$\begin{aligned} \text{ATLAS}: \mu_{\gamma\gamma}^{\text{ATLAS}} &= 1.09 \pm 0.09, \\ \text{CMS}: \quad \mu_{\gamma\gamma}^{\text{CMS}} &= 1.13 \pm 0.09. \end{aligned} \tag{62}$$

The dominant production mechanism for the Higgs boson is gluon-gluon fusion, mediated by a top quark loop. Because the coupling of the SM-like Higgs boson to fermions is normalized to the SM values by Eq. (59), we obtain the following expression for the ratio of the Higgs production cross section in our model $\sigma(pp \to h)$ to the SM prediction $\sigma(pp \to h)_{\text{SM}}$

$$\frac{\sigma(pp \to h)}{\sigma(pp \to h)_{\text{SM}}} \simeq \left(\frac{\cos\gamma_2}{\sin(\gamma_2 - \gamma_1)} \right)^2. \tag{63}$$

The branching ratios, $\text{Br}\,(h_i \to \gamma\gamma)$, represent the probability of the Higgs boson (h_i) decaying into two photons $(\gamma\gamma)$. It is calculated as follows

$$\text{Br}\,(h_i \to \gamma\gamma) = \frac{\gamma(h_i \to \gamma\gamma)}{\gamma(h_i \to \text{all})}, \tag{64}$$

In the considered model, the couplings of light CP-even scalar Higgs boson, $h_1 \equiv h, h_2 \equiv h_{95}$, to two photons are determined from the Feynman diagrams given in Fig. 2 and the partial widths at

leading order (LO) are given as follow

$$\gamma(h_i \to \gamma\gamma) = \frac{G_F \alpha^2 m_{h_i}^3}{128\sqrt{2}\pi^3} \left| \sum_f N_c^f Q_f^2 \kappa_{h_i ff} A_{1/2}(\tau_f) + \sum_{V=W,X} \frac{m_W^2}{m_V^2} \kappa_{h_i VV} A_1(\tau_V) + \sum_{\phi_j} \frac{v}{2m_{\phi_j}^2} g_{h_i \phi_j \phi_j} A_0(\tau_\phi) \right|^2, \quad (65)$$

where $\tau_k = \frac{m_{h_i}^2}{4m_k^2}$ and the $A_i(\tau)$ functions have a following form

$$\begin{aligned} A_0(\tau) &= -\frac{\tau - f(\tau)}{\tau^2}, \\ A_{1/2}(\tau) &= \frac{2(\tau + (\tau-1)f(\tau))}{\tau^2}, \\ A_1(\tau) &= -\frac{2\tau^2 + 3\tau + 3(2r-1)f(\tau)}{\tau^2}, \end{aligned} \quad (66)$$

with the function $f(\tau)$ is determined as

$$f(\tau) = \begin{cases} \arcsin^2 \sqrt{\tau} & \text{if} \quad \tau \le 1 \\ -\frac{1}{4}\left[\log\left(\frac{1+\sqrt{1-\tau^{-1}}}{1-\sqrt{1-\tau^{-1}}}\right) - i\pi\right]^2 & \text{if} \quad \tau > 1 \end{cases} \quad (67)$$

It should be noted that the model contains a new heavy-charged Higgs boson $X_\mu^\pm$, beside the SM one $W_\mu^\pm$, see in [63, 64]. This gauge boson also contributes to $\gamma(h_i \to \gamma\gamma)$. However, this contribution is significantly suppressed by the factor $\frac{m_W^2}{m_X^2} \ll 1$ (shown in Eq. (65)) compared to SM contribution by $W_\mu^\pm$ since $m_X \sim \mathcal{O}(1)$ TeV much larger than m_W. Therefore, in the following numerical studies, we will ignore this kind of contribution.

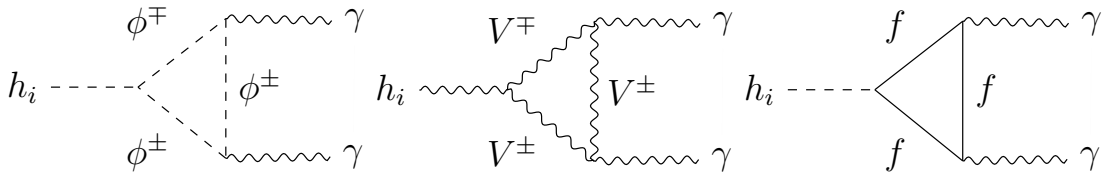

Fig. 2. 1-loop contribution to $h_i \to \gamma\gamma$. Here the first, middle, and third diagrams present the contribution of charged Higgs $\phi_j^\pm$, charged gauge bosons $V = W, X$, and fermion to decays $h_i \to \gamma\gamma$, respectively.

The total Higgs decay width is significantly summed over channels

$$\gamma(h_i \to \text{all}) = \sum_{f=b,c,\tau} \gamma\left(h_i \to f\bar{f}\right) + \sum_{V=W,Z} \gamma(h_i \to VV^*) + \gamma(h_i \to \gamma\gamma) + \gamma(h_i \to gg), \quad (68)$$

with

$$\begin{aligned}
\gamma(h_i \to f\bar{f}) &= N_c \frac{G_F m_{h_i} m_f^2}{4\sqrt{2}\pi} g_{h_i ff}^2, \\
\gamma(h_i \to VV^*) &= \frac{3G_F^2 m_V^4 m_{h_i}}{16\pi^3} \left(\frac{g_{h_i VV}}{g_{hVV}^{SM}}\right)^2 \delta_V R(x_i), \quad x_i = \frac{m_V^2}{m_{h_i}^2}, \\
\gamma(h_i \to gg) &= \frac{G_F \alpha_s^2 m_{h_i}^3}{36\sqrt{2}\pi^3} \left| \frac{3}{4} \sum_q \kappa_{hq\bar{q}} A_{1/2}(\tau_q) \right|^2,
\end{aligned} \tag{69}$$

where

$$\delta_W = 1, \quad \delta_Z = \frac{7}{12} - \frac{10}{9} s_W^2 + \frac{40}{27} s_W^4, \tag{70}$$

and the function $R(x)$ is defined by

$$\begin{aligned}
R(x) = {} & \frac{3\left(1-8x+20x^2\right)}{\sqrt{4x-1}} \arccos\left(\frac{3x-1}{2x\sqrt{x}}\right) - \frac{1-x}{2x}\left(2-13x+47x^2\right) \\
& -\frac{3}{2}\left(1-6x+4x^2\right)\ln x.
\end{aligned} \tag{71}$$

The SM-Higgs decay widths are obtained from those of the SM-like Higgs bosons in the limit: $g_{hH_i^+H_i^-} \to 0, \gamma_1 \to \frac{2\gamma_1+\pi}{4}$. The input parameters for estimating the signal strength are $u^2 + v^2 = (246\ \text{GeV})^2$, and other parameters are taken from Particle Data Group (PDG) [68]. The signal strength is respectively scanned for $g_{hH_2^+H_2^-} = 20\ \text{GeV}, 200\ \text{GeV}$ and 2000 GeV, where we ignore the contributions of the heavy charged Higgs bosons $H_{1,3,4}^\pm$ and the lightest charged Higgs mass $H_2^\pm$ is scanned for $m_{H_2^\pm} = 150\ \text{GeV}, 500\ \text{GeV}$. We consider the regions of mixing angles γ_1, γ_2 satisfying the experimental bounds given in Eq. (62).

From the Fig. 3, we see that for $m_{H_2^\pm} = 150$ GeV, the signal strength, $\mu_{\gamma\gamma}$, is sensitive to the choices of the couplings between the SM-like Higgs boson and the singly charged Higgs one $g_{hH_2^+H_2^-}$. Particularly, the regions fulfilled the CMS and ATLAS experimental constraints [68] expand when the coupling $g_{hH_2^+H_2^-}$ increases, except the case $g_{hH_2^+H_2^-} = 2000$ GeV, which generates the tiny region compared to other options $g_{hH_2^+H_2^-} = 20, 200$ GeV. On the other hand, for larger mass $m_{H_2^\pm} = 500$ GeV, the behavior changes notably. In such scenario, the regions that correspond to different values of $g_{hH_2^+H_2^-}$ are quite overlapped, especially the regions with $g_{hH_2^+H_2^-} = 20$ and 200 GeV , which are nearly identical. This indicates that the signal strength $\mu_{\gamma\gamma}$ is quite insensitive to the choice of $g_{hH_2^+H_2^-}$ in the scenario $m_{H_2^\pm} = 500$ GeV. We can explain this behavior for the following reasons. The contribution of charged Higgs boson to signal strength $\mu_{\gamma\gamma}$ depends on the factor $[v/(2m_{H_2^\pm}^2)] \times g_{hH_2^+H_2^-} \simeq 5.46 \times 10^{-3} g_{hH_2^+H_2^-}$ for $m_{H_2^\pm} = 150$ GeV, whereas $[v/(2m_{H_2^\pm}^2)] \times g_{hH_2^+H_2^-} \simeq 4.9 \times 10^{-4} g_{hH_2^+H_2^-}$ for $m_{H_2^\pm} = 500$ GeV which is remarkably smaller. Therefore, if the magnitude of coupling is $g_{hH_2^+H_2^-} \sim \mathcal{O}(10^1 - 10^3)$ GeV, the contribution of charged Higgs boson with mass $m_{H_2^\pm} = 500$ GeV will have a low order of magnitude $\mathcal{O}(10^{-3} - 10^{-1})$, which will not modify significantly to $\mu_{\gamma\gamma}$. Inversely, the case $m_{H_2^\pm} = 150$ GeV will induce the contribution with

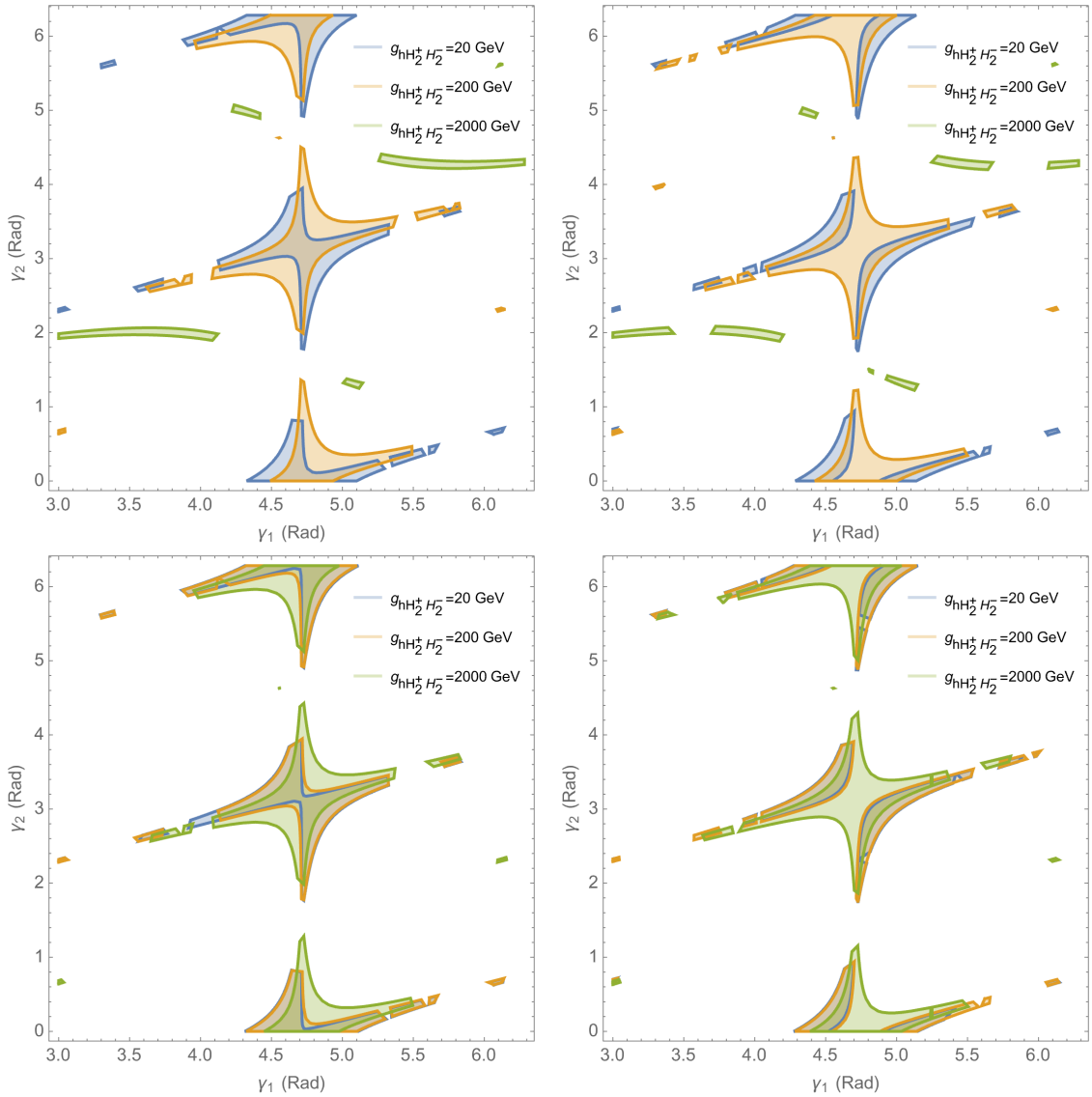

Fig. 3. The correlations between the mixing angles γ_1, γ_2 are consistent with the experimental constraints on the signal strength $\mu_{\gamma\gamma}$ [68]. The left and right panels show the regions satisfying the measurement by ATLAS and CMS, respectively. Besides, the top and bottom panels are plotted when fixing the mass of the lightest charged Higgs at $m_{H_2^\pm} = 150$ GeV and $m_{H_2^\pm} = 500$ GeV, respectively.

magnitude $\sim \mathcal{O}(10^{-2} - 10^{0})$, larger 10 times compared to case $m_{H_2^\pm} = 500$ GeV. Consequently, the panels with $m_{H_2^\pm} = 500$ GeV are insensitive with values of couplings $g_{hH_2^+H_2^-}$ whereas the ones with $m_{H_2^\pm} = 150$ GeV show the stronger influence of $g_{hH_2^+H_2^-}$.

5. The 95 GeV diphoton excess

Let's investigate if the Higgs boson h_{95} can explain the experimental hint observed around 95 GeV. This requires determining the regions in the parameter space that would produce a diphoton signal strength for h_{95} consistent with the results reported in [17, 69]

$$\mu_{\gamma\gamma}^{h_{95}-\text{CMS}} = \frac{\sigma^{\text{CMS}}\left(gg \to h_{95} \to \gamma\gamma\right)}{\sigma^{\text{SM}}\left(gg \to h \to \gamma\gamma\right)} = 0.33^{+0.19}_{-0.12}. \tag{72}$$

In our theory, the diphoton signal strength for h_{95} is predicted as follows

$$\mu_{\gamma\gamma}^{h_{95}} = \frac{\sigma\left(gg \to h_{95}\right)}{\sigma\left(gg \to h\right)} \times \frac{\text{Br}\left(h_{95} \to \gamma\gamma\right)}{\text{Br}\left(h \to \gamma\gamma\right)} = \left(\frac{\cos\gamma_1}{\cos\gamma_2}\right)^2 \times \frac{\text{Br}\left(h_{95} \to \gamma\gamma\right)}{\text{Br}\left(h \to \gamma\gamma\right)}. \tag{73}$$

Assuming $m_{H_2^\pm} = 150$ GeV, Fig. 4 shows contours of $\mu_{\gamma\gamma}^{h_{95}}$ in the $\gamma_1 - \gamma_2$ plane for $g_{hH_2^+H_2^-} = 20, 200$ GeV. The results indicate that our model allows the region for the mixing angles γ_1, γ_2 that could accommodate the observed CMS diphoton excess [17, 69].

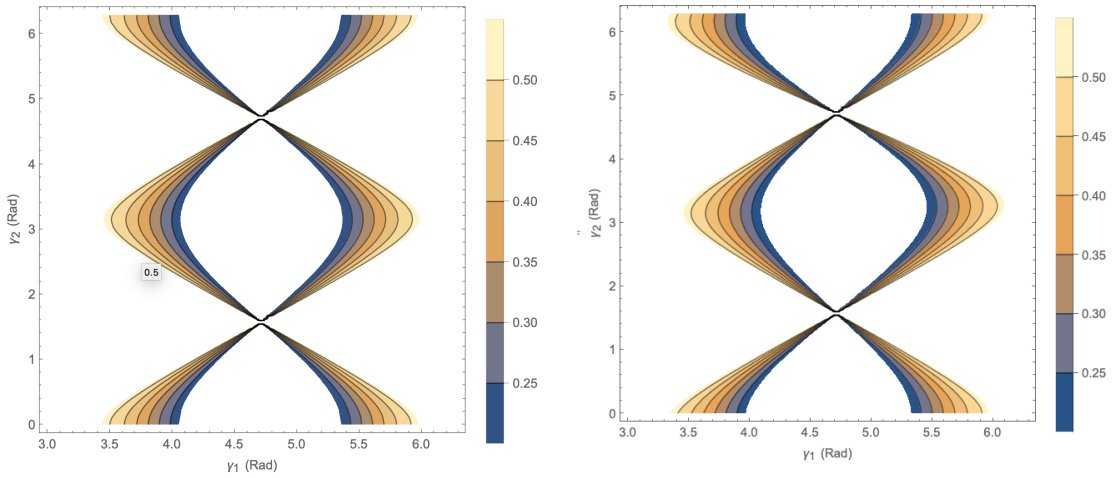

Fig. 4. Region of the $\gamma_1 - \gamma_2$ plane that explains the CMS 95 GeV diphoton excesses [17, 69] for taking $m_{H_2^\pm} = 150$ GeV. The left and right panels are plotted by fixing $g_{h_{95}H_2^+H_2^-} = 20$ GeV and $g_{h_{95}H_2^+H_2^-} = 2000$ GeV, respectively.

6. Conclusions

We have studied in a more detail the scalar sector in the considered model. The model possesses a sufficient number of massless particles to account for the longitudinal components of the massive vector boson. In addition to the SM-like Higgs boson, the model predicts two additional Higgs bosons at the electroweak scale: a neutral CP-even Higgs, and a singly charged Higgs one. The remaining scalar particles have masses depending on the new physical scale. The light even-scalar, h, aligns with the Higgs-like state discovered by the CMS and ATLAS in 2012 [1, 2]. The other, h_{95}, potentially explains the 95GeV hinted at by CMS data. The couplings

of the h to the SM fermion are normalized by factor $\kappa_{hVV} \sim \kappa_{hff} = \frac{\cos\gamma_1}{\sin(\gamma_2-\gamma 1)}$ and those of the h_{95} are normalized by factor $a_{hVV} \sim a_{hff} = \frac{\cos\gamma_2}{\sin(\gamma_2-\gamma_1)}$. We have demonstrated that the model can potentially explain both the main excesses observed in the scalar field at the LHC and the diphoton excess hinted at by CMS data around 95 GeV, within specific regions of mixing angles γ_1, γ_2.

Acknowledgment

N.T. Duy was funded by the Postdoctoral Scholarship Programme of Vingroup Innovation Foundation (VINIF), code VINIF.2023.STS.65.

References

[1] CMS collaboration, *Observation of a New Boson at a Mass of 125 GeV with the CMS Experiment at the LHC*, Phys. Lett. B **716** (2012) 30.
[2] ATLAS collaboration, *Observation of a new particle in the search for the Standard Model Higgs boson with the ATLAS detector at the LHC*, Phys. Lett. B **716** (2012) 1.
[3] OPAL collaboration, *Decay mode independent searches for new scalar bosons with the OPAL detector at LEP*, Eur. Phys. J. C **27** (2003) 311.
[4] LEP WORKING GROUP FOR HIGGS BOSON SEARCHES, ALEPH, DELPHI, L3, OPAL collaboration, *Search for the standard model Higgs boson at LEP*, Phys. Lett. B **565** (2003) 61.
[5] ALEPH, DELPHI, L3, OPAL, LEP WORKING GROUP FOR HIGGS BOSON SEARCHES collaboration, *Search for neutral MSSM Higgs bosons at LEP*, Eur. Phys. J. C **47** (2006) 547.
[6] CDF collaboration, *Search for Higgs bosons predicted in two-Higgs-doublet models via decays to tau lepton pairs in 1.96-TeV p anti-p collisions*, Phys. Rev. Lett. **103** (2009) 201801.
[7] CDF collaboration, *Search for Higgs Bosons Produced in Association with b-quarks*, Phys. Rev. D **85** (2012) 032005.
[8] D0 collaboration, *Search for Higgs bosons decaying to $\tau\tau$ pairs in $p\bar{p}$ collisions at $\sqrt{s} = 1.96$ TeV*, Phys. Lett. B **707** (2012) 323.
[9] D0 collaboration, *Search for Neutral Higgs Bosons in the Multi-b-Jet Topology in 5.2fb^{-1} of $p\bar{p}$ Collisions at $\sqrt{s} = 1.96$ TeV*, Phys. Lett. B **698** (2011) 97.
[10] CDF, D0 collaboration, *Updated Combination of CDF and D0 Searches for Standard Model Higgs Boson Production with up to 10.0 fb^{-1} of Data*, 7, 2012.
[11] CMS collaboration, *Search for neutral MSSM Higgs bosons decaying into a pair of bottom quarks*, J. High Energy Phys. **11** (2015) 071.
[12] CMS collaboration, *Search for beyond the standard model Higgs bosons decaying into a $\mathrm{b\bar{b}}$ pair in pp collisions at $\sqrt{s} = 13$ TeV*, J. High Energy Phys. **08** (2018) 113.
[13] ATLAS collaboration, *Search for additional heavy neutral Higgs and gauge bosons in the ditau final state produced in 36 fb^{-1} of pp collisions at $\sqrt{s} = 13$ TeV with the ATLAS detector*, J. High Energy Phys. **01** (2018) 055.
[14] CMS collaboration, *Searches for additional Higgs bosons and for vector leptoquarks in $\tau\tau$ final states in proton-proton collisions at $\sqrt{s} = 13$ TeV*, J. High Energy Phys. **07** (2023) 073.
[15] CMS collaboration, *Search for new resonances in the diphoton final state in the mass range between 80 and 115 GeV in pp collisions at $\sqrt{s} = 8$ TeV*, .
[16] CMS collaboration, *Search for a standard model-like Higgs boson in the mass range between 70 and 110 GeV in the diphoton final state in proton-proton collisions at $\sqrt{s} = 8$ and 13 TeV*, Phys. Lett. B **793** (2019) 320.
[17] CMS collaboration, *Search for a standard model-like Higgs boson in the mass range between 70 and 110* GeV *in the diphoton final state in proton-proton collisions at $\sqrt{s} = 13$* TeV, .
[18] T. D. Lee, *A Theory of Spontaneous T Violation*, Phys. Rev. D **8** (1973) 1226.
[19] G. C. Branco, P. M. Ferreira, L. Lavoura, M. N. Rebelo, M. Sher and J. P. Silva, *Theory and phenomenology of two-Higgs-doublet models*, Phys. Rept. **516** (2012) 1.

[20] J. F. Gunion and H. E. Haber, *The CP conserving two Higgs doublet model: The Approach to the decoupling limit*, Phys. Rev. D **67** (2003) 075019.

[21] I. P. Ivanov and E. Vdovin, *Classification of finite reparametrization symmetry groups in the three-Higgs-doublet model*, Eur. Phys. J. C **73** (2013) 2309.

[22] R. González Felipe, H. Serôdio and J. P. Silva, *Models with three Higgs doublets in the triplet representations of A_4 or S_4*, Phys. Rev. D **87** (2013) 055010.

[23] M. Maniatis, *The Next-to-Minimal Supersymmetric extension of the Standard Model reviewed*, Int. J. Mod. Phys. A **25** (2010) 3505.

[24] J. C. Pati and A. Salam, *Lepton Number as the Fourth Color*, Phys. Rev. D **10** (1974) 275.

[25] H. Georgi and S. L. Glashow, *Unity of All Elementary Particle Forces*, Phys. Rev. Lett. **32** (1974) 438.

[26] H. Fritzsch and P. Minkowski, *Unified Interactions of Leptons and Hadrons*, Annals Phys. **93** (1975) 193.

[27] R. W. Robinett and J. L. Rosner, *Mass Scales in Grand Unified Theories*, Phys. Rev. D **26** (1982) 2396.

[28] R. N. Mohapatra and J. C. Pati, *Left-Right Gauge Symmetry and an Isoconjugate Model of CP Violation*, Phys. Rev. D **11** (1975) 566.

[29] F. Pisano and V. Pleitez, *$SU(3) \times U(1)$ model for electroweak interactions*, Phys. Rev. D **46** (1992) 410.

[30] P. H. Frampton, *Chiral dilepton model and the flavor question*, Phys. Rev. Lett. **69** (1992) 2889.

[31] R. Foot, O. F. Hernández, F. Pisano and V. Pleitez, *Lepton masses in an $SU(3)_L \times U(1)_N$ gauge model*, Phys. Rev. D **47** (1993) 4158.

[32] M. Singer, J. W. F. Valle and J. Schechter, *Canonical neutral-current predictions from the weak-electromagnetic gauge group $su(3) \times u(1)$*, Phys. Rev. D **22** (1980) 738.

[33] J. C. Montero, F. Pisano and V. Pleitez, *Neutral currents and glashow-iliopoulos-maiani mechanism in $SU(3)_L \times U(1)_N$ models for electroweak interactions*, Phys. Rev. D **47** (1993) 2918.

[34] R. Foot, H. N. Long and T. A. Tran, *$SU(3)_L \times U(1)_N$ and $SU(4)_L \times U(1)_N$ gauge models with right-handed neutrinos*, Phys. Rev. D **50** (1994) R34.

[35] P. B. Pal, *The Strong CP question in SU(3)(C) x SU(3)(L) x U(1)(N) models*, Phys. Rev. D **52** (1995) 1659.

[36] A. G. Dias, C. A. de S. Pires and P. S. Rodrigues da Silva, *Discrete symmetries, invisible axion and lepton number symmetry in an economic 3 3 1 model*, Phys. Rev. D **68** (2003) 115009.

[37] A. G. Dias and V. Pleitez, *Stabilizing the invisible axion in 3-3-1 models*, Phys. Rev. D **69** (2004) 077702.

[38] F. Pisano, *A Simple solution for the flavor question*, Mod. Phys. Lett. A **11** (1996) 2639.

[39] A. Doff and F. Pisano, *Charge quantization in the largest leptoquark bilepton chiral electroweak scheme*, Mod. Phys. Lett. A **14** (1999) 1133.

[40] C. A. de Sousa Pires, *Remark on the vector - like nature of the electromagnetism and the electric charge quantization*, Phys. Rev. D **60** (1999) 075013.

[41] P. V. Dong and H. N. Long, *Electric charge quantization in SU(3)(C) x SU(3)(L) x U(1)(X) models*, Int. J. Mod. Phys. A **21** (2006) 6677.

[42] D. Fregolente and M. D. Tonasse, *Selfinteracting dark matter from an SU(3)(L) x U(1)(N) electroweak model*, Phys. Lett. B **555** (2003) 7.

[43] H. N. Long and N. Q. Lan, *Selfinteracting dark matter and Higgs bosons in the SU(3)(C) x SU(3)(L) x U(1)(N) model with right-handed neutrinos*, EPL **64** (2003) 571.

[44] S. Filippi, W. A. Ponce and L. A. Sanchez, *Dark matter from the scalar sector of 3-3-1 models without exotic electric charges*, EPL **73** (2006) 142.

[45] P. V. Dong, D. T. Huong, F. S. Queiroz, J. W. F. Valle and C. A. Vaquera-Araujo, *The Dark Side of Flipped Trinification*, J. High Energy Phys. **04** (2018) 143.

[46] M. B. Tully and G. C. Joshi, *Generating neutrino mass in the 331 model*, Phys. Rev. D **64** (2001) 011301.

[47] A. G. Dias, C. A. de S. Pires and P. S. Rodrigues da Silva, *Naturally light right-handed neutrinos in a 3-3-1 model*, Phys. Lett. B **628** (2005) 85.

[48] D. Chang and H. N. Long, *Interesting radiative patterns of neutrino mass in an SU(3)(C) x SU(3)(L) x U(1)(X) model with right-handed neutrinos*, Phys. Rev. D **73** (2006) 053006.

[49] D. T. Huong, P. V. Dong, C. S. Kim and N. T. Thuy, *Inflation and leptogenesis in the 3-3-1-1 model*, Phys. Rev. D **91** (2015) 055023.

[50] P. Van Dong, D. T. Huong, D. A. Camargo, F. S. Queiroz and J. W. F. Valle, *Asymmetric Dark Matter, Inflation and Leptogenesis from $B-L$ Symmetry Breaking*, Phys. Rev. D **99** (2019) 055040.

[51] P. V. Dong, D. Q. Phong, D. V. Soa and N. C. Thao, *The economical 3-3-1 model revisited*, Eur. Phys. J. C **78** (2018) 653.
[52] R. M. Fonseca and M. Hirsch, *A flipped 331 model*, J. High Energy Phys. **08** (2016) 003.
[53] D. Ng, *The Electroweak theory of SU(3) x U(1)*, Phys. Rev. D **49** (1994) 4805.
[54] D. Gomez Dumm, F. Pisano and V. Pleitez, *Flavor changing neutral currents in SU(3) x U(1) models*, Mod. Phys. Lett. A **9** (1994) 1609.
[55] H. N. Long and V. T. Van, *Quark family discrimination and flavor changing neutral currents in the SU(3)(C) x SU(3)(L) x U(1) model with right-handed neutrinos*, J. Phys. G **25** (1999) 2319.
[56] A. J. Buras, F. De Fazio, J. Girrbach and M. V. Carlucci, *The Anatomy of Quark Flavour Observables in 331 Models in the Flavour Precision Era*, J. High Energy Phys. **02** (2013) 023.
[57] A. J. Buras, F. De Fazio and J. Girrbach, *331 models facing new $b \to s\mu^+\mu^-$ data*, J. High Energy Phys. **02** (2014) 112.
[58] R. Gauld, F. Goertz and U. Haisch, *An explicit Z'-boson explanation of the $B \to K^*\mu^+\mu^-$ anomaly*, J. High Energy Phys. **01** (2014) 069.
[59] A. J. Buras and F. De Fazio, *ε'/ε in 331 Models*, J. High Energy Phys. **03** (2016) 010.
[60] P. Van Dong, N. T. K. Ngan, T. D. Tham, L. D. Thien and N. T. Thuy, *Phenomenology of the simple 3-3-1 model with inert scalars*, Phys. Rev. D **99** (2019) 095031.
[61] P. N. Thu, N. T. Duy, A. E. Carcamo Hernandez and D. T. Huong, *Lepton universality violation in the MF331 model*, arXiv:2304.03003.
[62] N. T. Duy, P. N. Thu and D. T. Huong, *New physics in $b \to s$ transitions in the MF331 model*, Eur. Phys. J. C **82** (2022) 966.
[63] D. T. Huong, D. N. Dinh, L. D. Thien and P. Van Dong, *Dark matter and flavor changing in the flipped 3-3-1 model*, J. High Energy Phys. **08** (2019) 051.
[64] T. T. Hong, H. T. Hung, H. H. Phuong, L. T. T. Phuong and L. T. Hue, *Lepton-flavor-violating decays of the SM-like Higgs boson $h \to e_i e_j$, and $e_i \to e_j \gamma$ in a flipped 3-3-1 model*, PTEP **2020** (2020) 043B03.
[65] CMS collaboration, *Combined measurements of Higgs boson couplings in proton–proton collisions at $\sqrt{s} = 13\,TeV$*, Eur. Phys. J. C **79** (2019) 421.
[66] ATLAS collaboration, *A detailed map of Higgs boson interactions by the ATLAS experiment ten years after the discovery*, Nature **607** (2022) 52.
[67] CMS collaboration, *A portrait of the Higgs boson by the CMS experiment ten years after the discovery.*, Nature **607** (2022) 60.
[68] PARTICLE DATA GROUP collaboration, *Review of Particle Physics*, PTEP **2022** (2022) 083C01.
[69] T. Biekötter, S. Heinemeyer and G. Weiglein, *The CMS di-photon excess at 95 GeV in view of the LHC Run 2 results*, Phys. Lett. B **846** (2023) 138217.